

SUPPORTING INFORMATION

A wafer-scale Bernal-stacked bilayer graphene film obtained on a dilute Cu(0.61 at% Ni) foil using atmospheric pressure chemical vapour deposition

M. J. Madito, N. Manyala*, A. Bello, J. K. Dangbegnon, T. M. Masikhwa and D. Y. Momodu

Department of Physics, Institute of Applied Materials, SARCHI Chair in Carbon Technology and Materials, University of Pretoria, Pretoria 0028, South Africa

* Corresponding Author: Tel: +27 (0)12 420 3549 and E-mail address: ncholu.manyala@up.ac.za (N. Manyala)

SEM and Raman data of monolayer graphene obtained on a pure Cu foil

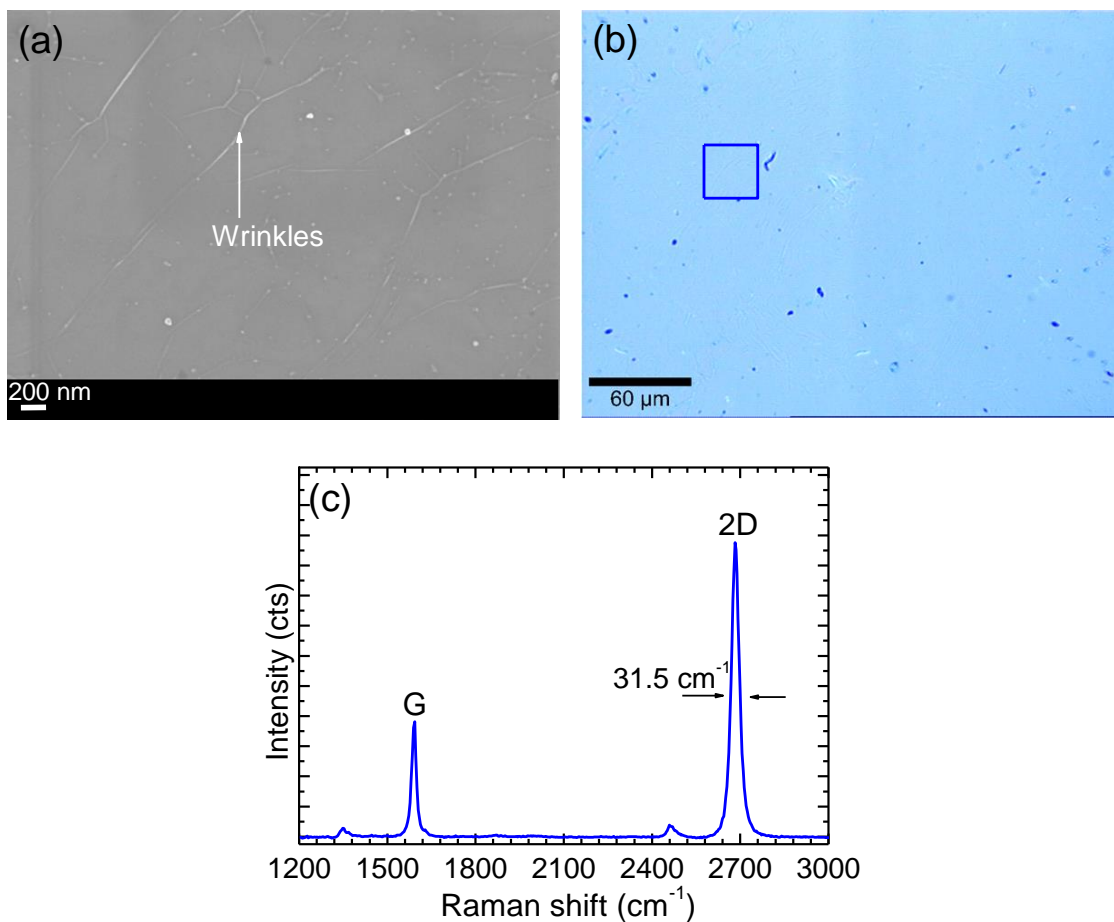


Figure S1. (a) SEM micrograph of a monolayer graphene film transferred onto 300 nm SiO₂/Si substrate. (b) Raman optical microscope image of monolayer graphene film on 300 nm SiO₂/Si substrate and the corresponding (c) average Raman spectra of spectra acquired from 30 μm² area (indicated with a square box in figure S1(b)) of a monolayer graphene film.

A monolayer graphene film on Cu foil was obtained from a mixture of Ar (300sccm), H₂ (9 sccm) and CH₄ (15 sccm) for 2 min at a growth temperature of 1000 °C.

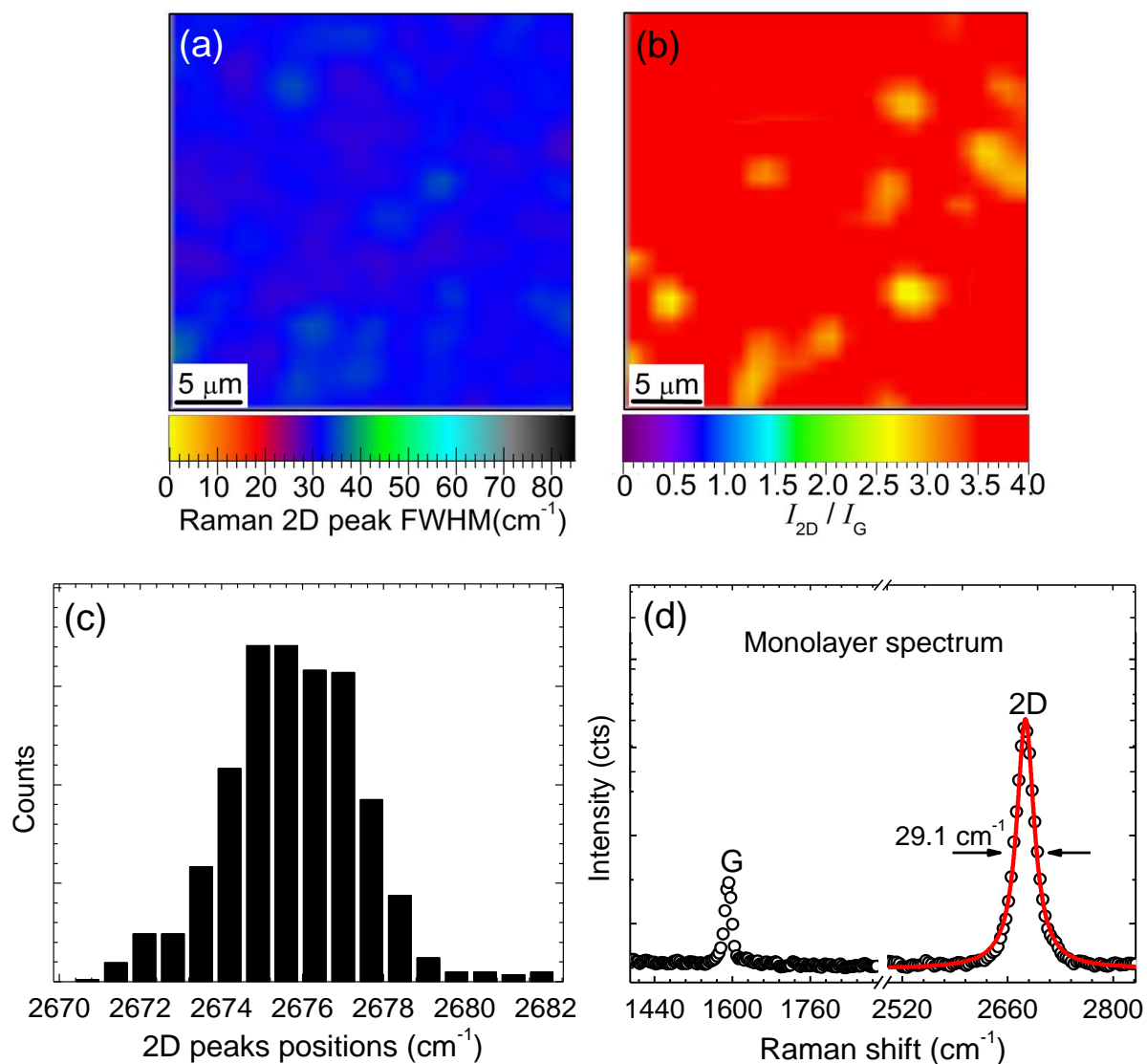


Figure S2. (a) The mapping of 2D peaks FWHMs and of the corresponding (b) 2D to G peaks intensities ratio (I_{2D}/I_G) for monolayer graphene film transferred onto 300 nm SiO_2/Si substrate. (c) The distribution of the 2D peak positions. (d) Raman spectrum from data mapped in figure S2(a) and the 2D peak solid-line is Lorentzian fit.

Table S1. Analysis results of Raman spectra of monolayer graphene film obtained on Cu foil substrate and transferred onto 300 nm SiO_2/Si for characterization.

Graphene	CVD substrate	2D peaks		2D/G peaks
		Position (cm^{-1})	FWHM (cm^{-1})	
Monolayer	Cu	2670–2682	28–36	2.5–4

SEM and Raman data of bilayer graphene obtained on a pure Cu foil

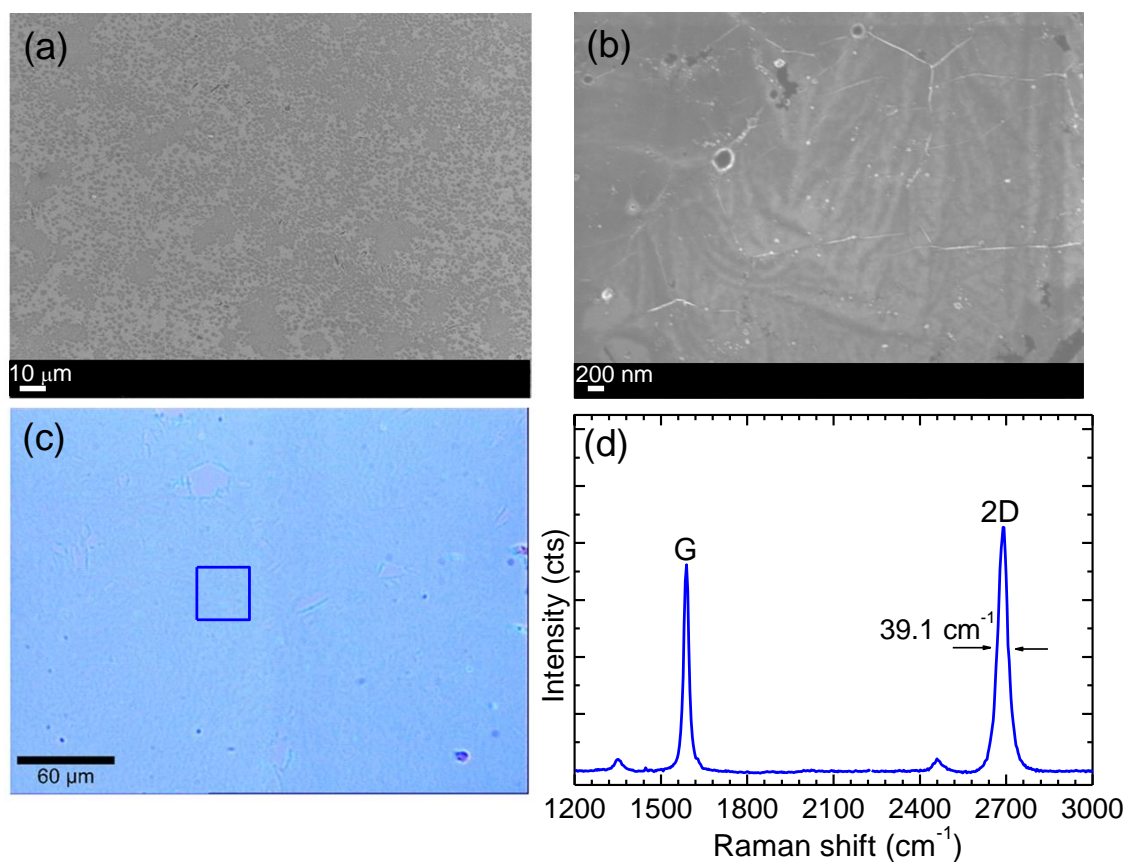


Figure S3. (a-b) SEM micrographs of a bilayer graphene film (at low and high magnifications respectively) transferred onto 300 nm SiO₂/Si substrate. (c) Raman optical microscope image of bilayer graphene film on 300 nm SiO₂/Si substrate and the corresponding (d) average Raman spectra of spectra acquired from 30 μm² area (indicated with a square box in figure S3(c)) of a bilayer graphene film.

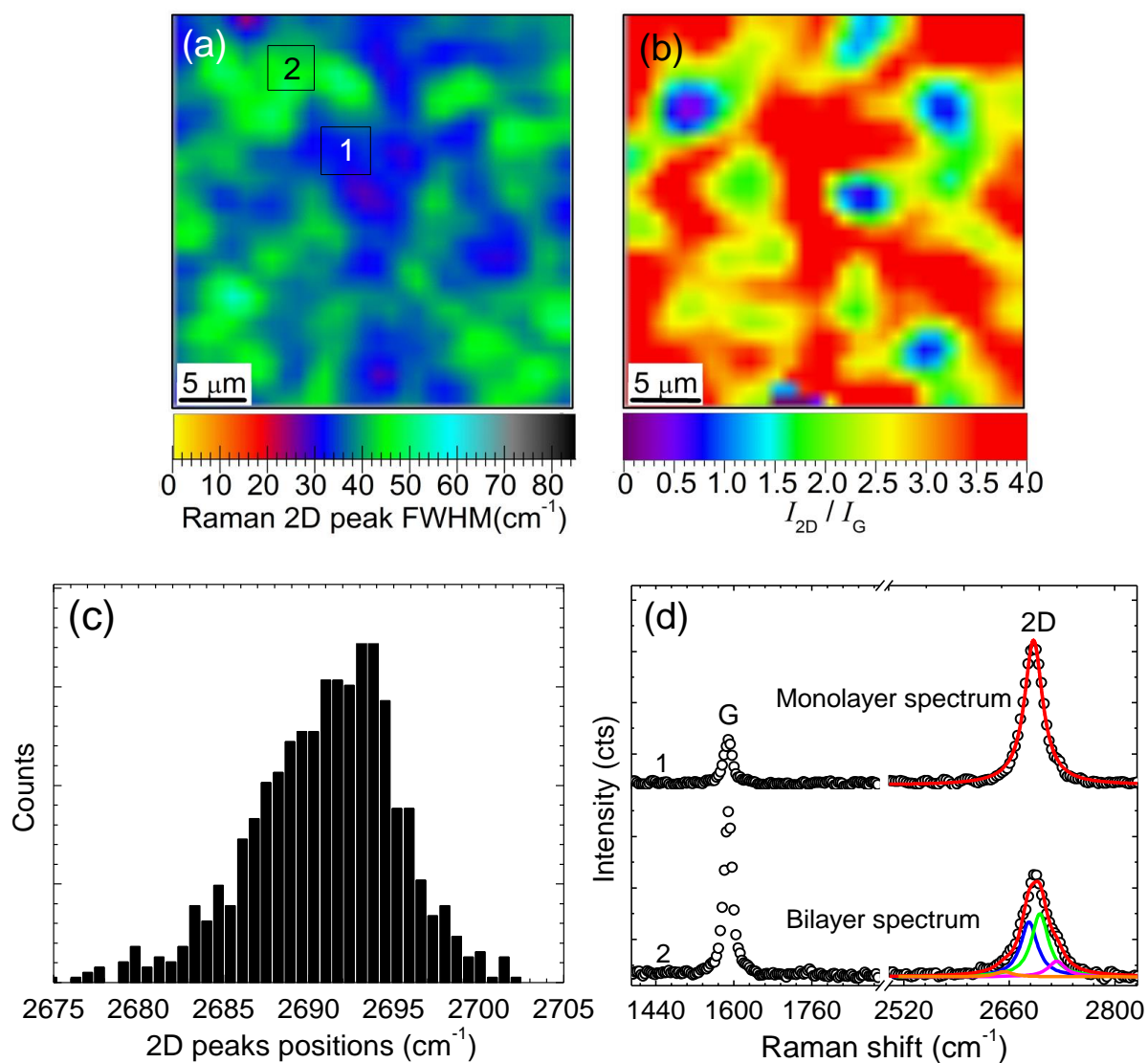


Figure S4. (a) The mapping of 2D peaks FWHMs and of the corresponding (b) 2D to G peaks intensities ratio (I_{2D}/I_G) for bilayer graphene film transferred onto 300 nm SiO_2/Si substrate. (c) The distribution of the 2D peaks positions. (d) Raman spectrum 1 and 2 are from area 1 and 2 in figure S4(a) respectively and the 2D peaks solid-lines are Lorentzians fits.

Table S2. Analysis results of Raman spectra of bilayer graphene film obtained on Cu foil substrate and transferred onto 300 nm SiO_2/Si for characterization.

Graphene	CVD substrate	2D peaks		2D/G peaks
		Position (cm^{-1})	FWHM (cm^{-1})	
Bilayer	Cu	2675–2703	28–53	0.8–4

SEM and Raman data of bilayer graphene obtained on Cu(0.61 at% Ni) foil

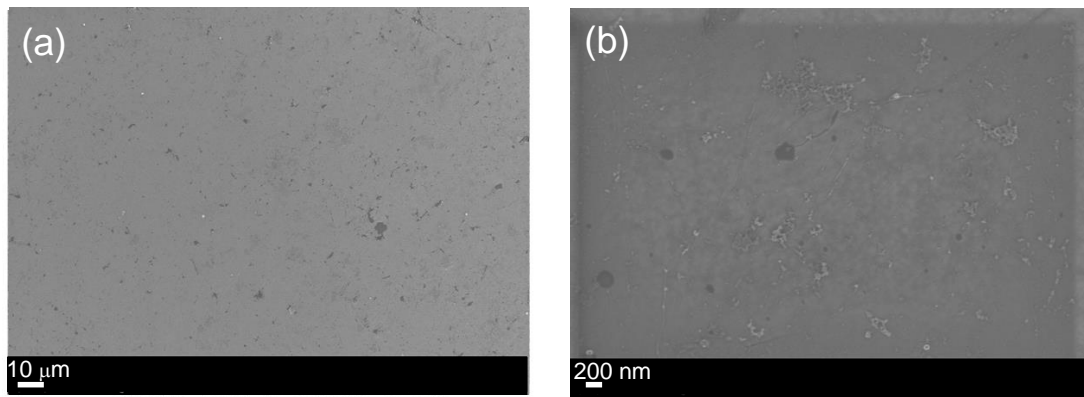


Figure S5. (a-b) SEM micrographs of a bilayer graphene film (at low and high magnifications respectively) transferred onto 300 nm SiO₂/Si substrate.

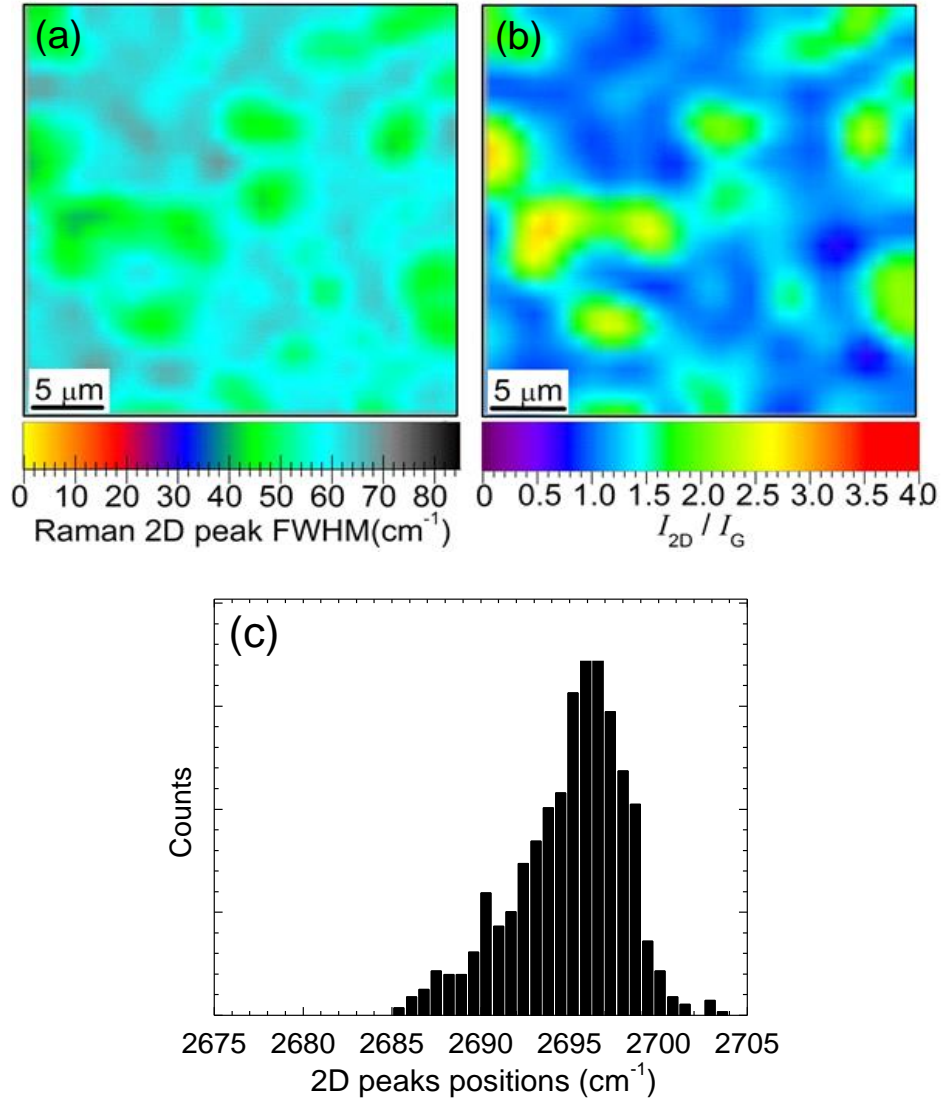


Figure S6. (a) The mapping of 2D peaks FWHMs and of the corresponding (b) 2D to G peaks intensities ratio (I_{2D}/I_G) for bilayer graphene film obtained on Cu(0.61 at% Ni) foil and transferred onto 300 nm SiO₂/Si substrate. (c) The distribution of the 2D peaks positions.

Table S3. Analysis results of Raman spectra of bilayer graphene film obtained on Cu(0.61 at% Ni) foil substrate and transferred onto 300 nm SiO₂/Si for characterization.

Graphene	CVD substrate	2D peaks		2D/G peaks
		Position (cm ⁻¹)	FWHM (cm ⁻¹)	
Bilayer	Cu(0.61 at% Ni)	2685–2703	38–70	0.8–2.5

TEM and SAED images of bilayer graphene film obtained on Cu(0.61 at% Ni) foil

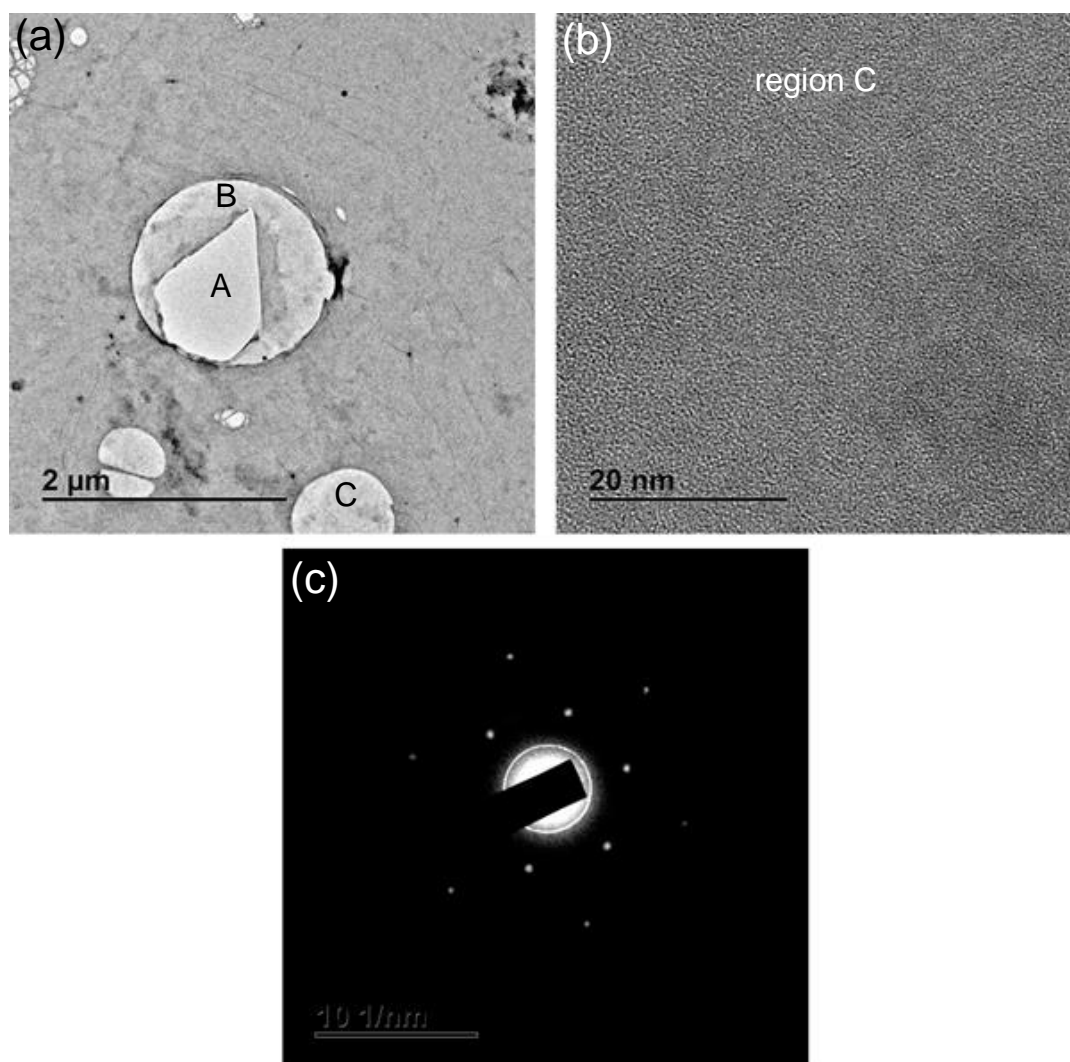


Figure S7. (a) Low magnification TEM image of bilayer graphene film obtained on Cu(0.61 at% Ni) foil and transferred on a lacey carbon TEM grid (region A, B and C shown in holes of a lacey carbon TEM grid show an area without graphene (A) and with graphene (B and C). (b) A high magnification TEM image of graphene in region C of figure (a). (c) A selected area electron diffraction pattern from an area shown in figure (b) and shows two sets of hexagonal diffraction spots.

Sheet resistance of monolayer (1LG) and bilayer (2LG) graphene films obtained on Cu and Cu(0.61 at% Ni) foils

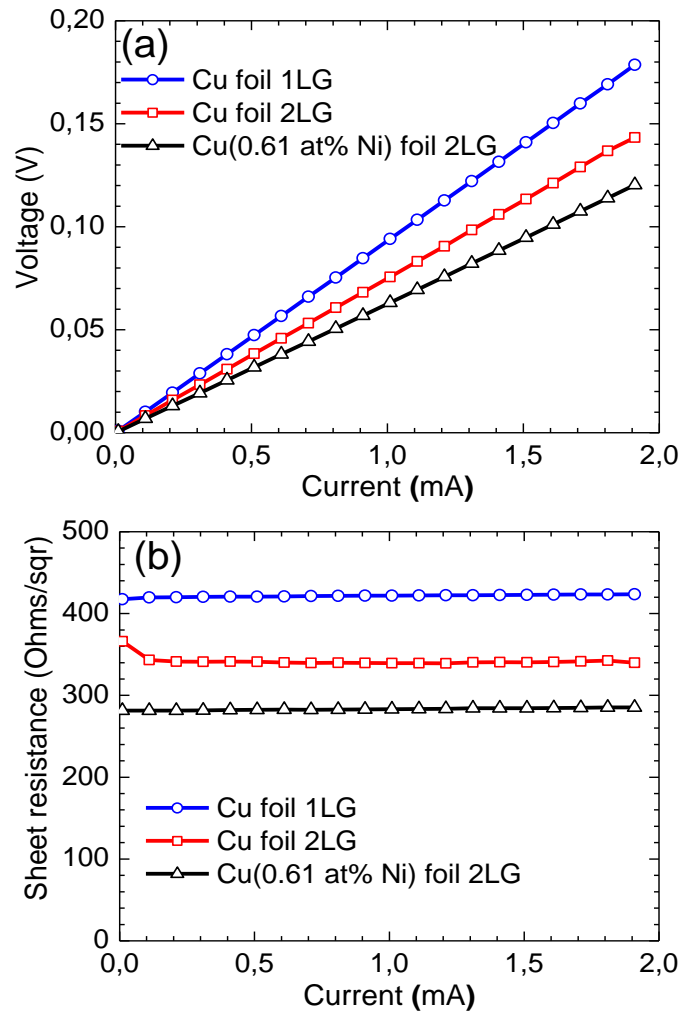


Figure S8. (a) A four-point probe measured voltage drop and (b) the corresponding sheet resistance of monolayer (1LG) and bilayer (2LG) graphene films obtained on Cu and dilute Cu(0.61 at% Ni) foils and transferred onto SiO₂/Si substrates.

Ni surface concentration in Cu(0.61 at% Ni) catalyst during AP-CVD graphene growth

During CVD graphene growth, a catalyst temperature is increased at a constant heating rate from room temperature to the desired growth temperature, and immediately after growth the temperature of the graphene/catalyst is decreased rapidly to room temperature. In a dilute Cu(0.61 at% Ni) catalyst, a temperature increase results in bulk-to-surface diffusion of Ni (due to the dependence on the Arrhenius term) which increases the surface concentration of Ni in the catalyst foil. Such increase in the surface concentration of Ni could be well-described by a semi-infinite solution of Fick's diffusion equation¹. In the semi-infinite solution of Fick, the surface enrichment factor (β) at temperature, T , is given by

$$\beta(T) = \frac{X^S(T) - X^B}{X^B} \quad (1)$$

where $X^S(T)$ is the surface concentration at temperature, T and X^B is the bulk concentration of the diffusing solute atoms ($X^B = 0.61$ at% in a dilute Cu(0.61 at% Ni) catalyst).

The temperature dependence of the enrichment factor in the semi-infinite solution of Fick is given by¹

$$\frac{X^S(T) - X^B}{X^B} = \left\{ \frac{4D_0}{\pi\alpha d^2} \left[\frac{RT^2}{Q} \exp(-Q/RT) \right] \right\}^{\frac{1}{2}} \quad (2)$$

where D_0 is the pre-exponential factor, Q is the activation energy ($D_0 = 7.0 \times 10^{-5} \text{ m}^2/\text{s}$, $Q = 225.0 \text{ kJ/mol}$ for Ni diffusion in Cu^2), α is the constant heating rate, d is interlayer distance ($d = 0.181 \text{ nm}$ in $\text{Cu}(001)$), R is the gas constant and T is the crystal temperature.

Equation 2 could well describe the temperature dependence of the surface concentration of Ni in dilute Cu(0.61 at% Ni) catalyst, however, cannot describe the temperature dependence of the maximum (or equilibrium) surface concentration of Ni in a catalyst. Nonetheless, the temperature dependence of the maximum surface concentration of Ni in a catalyst could be well-described by the well-known Langmuir–McLean equation^{1,3}:

$$\frac{X^\phi(T)}{1 - X^\phi(T)} = \frac{X^B}{1 - X^B} \exp(-\Delta G/RT) \quad (3)$$

where $X^\phi(T)$ is the relative surface concentration at temperature, T , $X^\phi(T) = \frac{X^s(T)}{X^M}$, X^M is the attainable maximum surface concentration ($X^M = 25$ at% in Cu(001)⁴) of solute atoms in the crystal surface, ΔG is the segregation energy.

Generally, $\Delta G = \Delta H - T\Delta S$, where ΔH is the segregation enthalpy, T is the temperature and ΔS is the segregation entropy. In dilute alloys, ΔS is negligible hence $\Delta G \approx \Delta H$ and the segregation enthalpy can be approximated by^{5,6}

$$\Delta H = \left(\frac{\Delta Z}{Z} \right) (\Delta H_B^{sub} - \Delta H_A^{sub}) \quad (4)$$

where Z is the bulk coordination number ($Z = 12$ for Cu crystal), ΔZ is the difference in coordination number between bulk and surface ($\Delta Z = 4$ for Cu(001)), ΔH^{sub} is the heat of sublimation for element A and B ($\Delta H_{Cu}^{sub} = 339.3$ kJ/mol, $\Delta H_{Ni}^{sub} = 430.1$ kJ/mol and $\Delta H_C^{sub} = 521.7$ kJ/mol⁷).

Following from equation 4, the segregation energy for Ni in Cu(001) surface is $\Delta G = 30.3$ kJ/mol. Now, using the semi-infinite solution of Fick (equation 2) and the Langmuir–McLean equation (equation 3), a view of the temperature dependence of the Ni surface concentration in a dilute Cu(0.61 at% Ni) catalyst during AP-CVD graphene growth was obtained as shown in figure S9. In figure S9, an increase in catalyst temperature increases the surface concentration of Ni (described by Fick solid-line) until it reaches a maximum (or equilibrium) surface concentration of 8.1 at% (determined by Fick and Langmuir–McLean solid-lines intersection) and a further increase in temperature result in a decrease in surface concentration of Ni due to surface-to-bulk diffusion of Ni or due to the sublimation of Ni, but at these catalyst temperatures (<1000 °C) and higher background pressure (atmospheric pressure) the sublimation of Ni (and Cu) is suppressed. At a CVD growth temperature of 980 °C a surface concentration of Ni is 2.1 at% in Cu(0.61 at% Ni) catalyst.

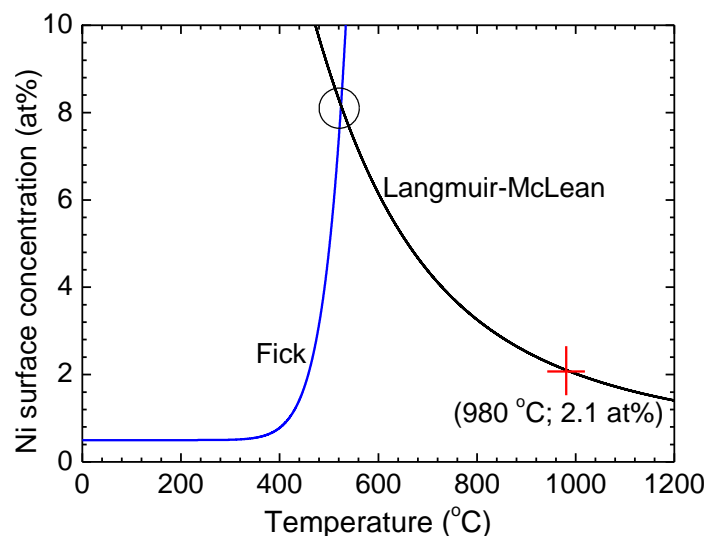


Figure S9. An illustration of the temperature dependence of the Ni surface concentration in a dilute Cu(0.61 at% Ni) catalyst at a constant heating rate of $\alpha = 0.5$ °C/s.

References

- 1 E. C. Viljoen and J. du Plessis, *Surface Science*, 1999, **431**, 128–137.
- 2 W. F. Gale and T. C. Totemeier, Eds., *Smithells Metals Reference Book*, Butterworth-Heinemann, Oxford UK, 8th edn., 2004.
- 3 D. R. Harries and A. D. Marwick, *Philosophical Transactions of the Royal Society A: Mathematical, Physical and Engineering Sciences*, 1980, **295**, 197–207.
- 4 E. C. Viljoen and J. du Plessis, *Surface Science*, 2000, **468**, 27–36.
- 5 K. Wandelt and C. R. Brundle, *Physical Review Letters*, 1981, **46**, 1529–1532.
- 6 S. Hofmann, R. Frech and W. Germany, *Analytical Chemistry*, 1985, **57**, 716–719.
- 7 D. R. Lide, *CRC Handbook of Chemistry and Physics*, CRC Press, Inc., 63rd edn., 2005.